

Raman spectroscopic and electrochemical studies of lithium battery components

D.E. Irish, Z. Deng, M. Odziemkowski

Department of Chemistry, University of Waterloo, Waterloo, Ont. N2L 3G1, Canada

Abstract

The species in the electrolyte and at, or near, the working electrode surface of an operating cell can be identified by Raman spectroscopy. Examples for the electrolyte methyl acetate/LiAsF₆, without and with CO₂ saturation, are described. The role of the additive, tetramethylammonium, is suggested. Conclusions from measurements of corrosion potential–time transients following in situ cutting to expose bare lithium metal to various organic electrolyte environments are reviewed. Preliminary Raman spectral measurements of carbon–coke anodes suggest that charging cycles cause intraplanar rupturing, thus reducing the microcrystallite size and causing measurable disorder.

Keywords: Lithium batteries; Raman spectroscopy

1. Introduction

Raman spectroscopy, coupled with electrochemistry, is a powerful tool for the study of species and processes occurring in model galvanic cells. The Raman spectrum provides vibrational frequencies, intensities, and other band parameters that often allow one to identify the species present in the electrolyte and those which adsorb to the electrode [1]. The ability to monitor the electrode/electrolyte interphase in situ while under potentiostatic/galvanostatic and environmental control is a major point in favour of Raman spectroscopy. In practice, the films on electrodes may be light or heat sensitive and decomposition under the laser beam, especially when focussed by a microscope, can be a problem. Also, the films may be insufficient to allow detection by normal Raman spectroscopy (NRS), which is an inherently weak effect. Surface-enhanced Raman scattering (SERS) allows detection of submonolayers under certain conditions; however, the working electrode is restricted to those free electron metals that support SERS—particularly silver, gold, and copper. Although lithium is potentially a SERS-active metal and reports of SERS from lithium in ultrahigh vacuum (UHV) have been reported [2], it is unlikely that such experiments will be successful in an electrochemical environment. Reasons for this and contributions realized from this spectroscopy are discussed below.

2. Experimental

Raman spectra have been recorded with a Dilor OMARS-89 spectrometer equipped with an intensified diode array detector; both macrochamber and microscope sampling arrangements have been employed. Excitation was achieved with the 514.53 nm line from a Coherent Innova 70 argon ion laser. Some solution spectra were recorded with a Jarrell-Ash 25-100 1.0 m Czerny-Turner monochromator equipped with a Model 129 digital cosecant stepping drive, an RCA 31034 selected photomultiplier tube, and an SSR Model 1104/1120 photon-counting system. Electrochemical measurements were made with a PAR Model 273 potentiostat/galvanostat.

3. Results and discussion

3.1. Electrolyte

In order to understand the phenomena that occur at or near the electrode surface, it is necessary to know what species exists in the electrolyte solution. In solutions of LiAsF₆ in methyl acetate (MA), the Raman spectrum reveals two sets of bands; one set is characteristic of the bulk solvent and the other set consists of bands that are shifted because they arise from

molecules solvating the lithium cation, and are thus perturbed by the ion-dipole interactions [3]. In Fig. 1, differences between the spectrum of the neat liquid MA (Fig. 1(a)) and the 1 M LiAsF₆/MA solution (Fig. 1(b)) are clearly visible. In particular, we have used the signal at 864 cm⁻¹ arising from the C-C stretching vibration of MA solvating the lithium cations, to measure the solvation number and to probe for the existence of Li⁺ near or on the electrode surface [4]. From the analysis of Raman band intensities for a range of compositions, it has been concluded that the solvation number of lithium is four [3]. In fact, four is a commonly found value for the small lithium ion. Four has been found for Li⁺ when solvated in acetone [5], acetonitrile [6,7], and ethylene carbonate [8]. The spectra also show that some small fractions of the AsF₆⁻ ions are ion-paired to Li⁺ in MA and that this fraction decreases with increase of bulk solvent dielectric constant [3].

3.2. Lithium/electrolyte interface

Attempts to identify the passive surface film(s) on lithium metal by SERS have so far been unsuccessful. For a successful SERS experiment, one would traditionally start with a clean metal surface, roughen that surface by a controlled oxidation/reduction cycle and monitor that surface in the double-layer region of the potential range at potentials from positive of the point of zero charge (pzc) to negative of it. Such experiments have been done for gold, silver and copper electrodes for a wide range of solution composition, pH, and laser wavelength values [9,10]. Lithium cannot be created 'clean' in an electrochemical environment. A passive film is always present. Guillotine experiments, designed to create a bare lithium surface, reveal that the surface film reforms 'completely' in less than 1 s [11,12]. The resulting films are too thick to support SERS and often too laser sensitive to give NRS. Some information has been obtained by measuring corrosion potential-time transients. These permit the ranking of the reactivity of electrolytes. For purified solvents, the results suggest

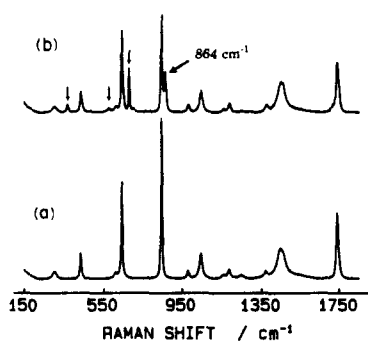


Fig. 1. Raman spectra of (a) pure methyl acetate (MA) and (b) 1 M LiAsF₆/MA in the 150–1850 cm⁻¹ region. Arrows designate bands of AsF₆⁻. The 864 cm⁻¹ band of Li(MA)₄⁺ is marked.

that the solvents tetrahydrofuran (THF), 2-methyltetrahydrofuran (2Me-THF) and propylene carbonate (PC) are 'stable' when compared with the AsF₆⁻ anion; reduction of this species overshadows any possible solvent reduction reaction [11]. This conclusion is consistent with that of Campbell et al. [13], viz., films formed on lithium surfaces are formed in most cases by electrochemical reduction of the electrolyte anions.

Other salts investigated—LiBF₄, LiClO₄ and Li(CF₃SO₂)₂N—showed much less reactivity towards the bare lithium when compared with the LiAsF₆. Comparison of three solvents, PC, 2Me-THF and THF, containing 0.6 M Li(CF₃SO₂)₂N or 0.6 M LiClO₄ (Fig. 2) indicated that PC shows the highest reactivity versus bare lithium metal. Corrosion potentials are initially much larger when water impurity (300 to 3000 ppm) exists (Fig. 3); water appears to lead to breakdown of the surface film and thus a brief exposure of bare lithium metal during intense anodic cycling [12].

3.3. In situ Raman spectral measurements of a 'model' system

Because lithium metal does not support electrochemical SERS, for the reasons described above, measurements have been made with a noble metal working electrode, silver, in methyl acetate (MA) containing 0.1 M LiAsF₆. The surface chemistry of lithium in lithium salt solutions of non-aqueous organic solvents has been reported to be similar to that of noble metal electrodes polarized to low potentials [14,15]. Thus, the use of silver may reveal the sort of processes which occur at or near the lithium electrode surface. Methyl acetate has been proposed as a possible lithium battery solvent [16–19]; saturation with CO₂ significantly increases the lithium-cycling efficiency [20]. We have thus chosen MA for this study and also report on the effect on the Raman spectra of saturation of the electrolyte with CO₂.

In order to achieve a SERS-active silver surface, it is necessary to roughen the electrode by an oxidation/reduction cycle, usually in the presence of a halide ion. Tetramethylammonium bromide (0.005 M) was introduced for this purpose. The bromide ion also served as a component of the Ag|AgBr|Br⁻ reference electrode. A platinum counter electrode was used. Addition to the electrolyte of tetraalkylammonium salts has been reported to significantly improve the stability of high rate lithium batteries [21]. The results of this study rationalize this claim.

Following the oxidation/reduction cycle, a signal at 859 cm⁻¹ characteristic of solvated lithium cations was clearly detected, indicating that these cations were adsorbed through a layer of bromide ions to the positive electrode surface [4]. As the potential was swept towards the pzc, the signal from Li(MA)₄⁺ diminished, as did

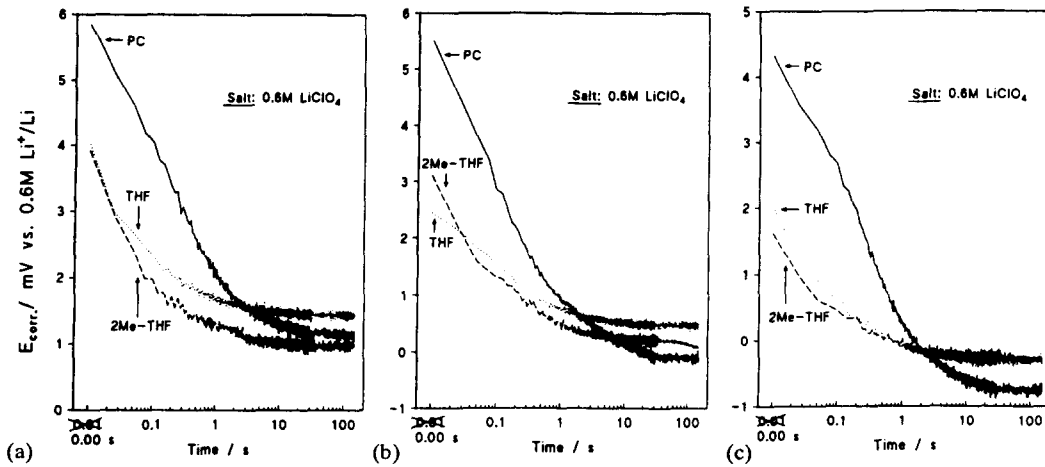
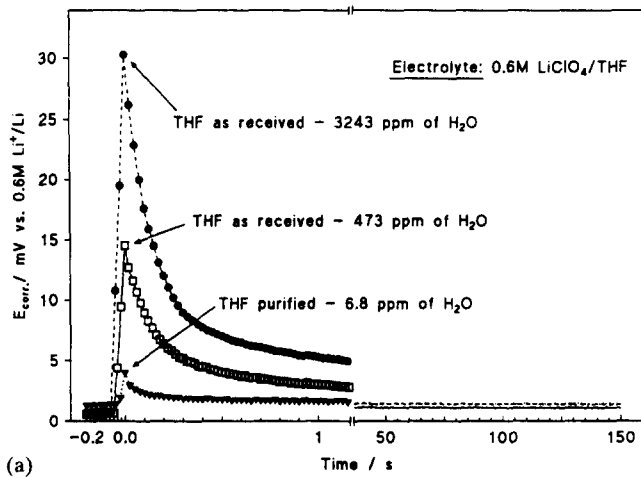
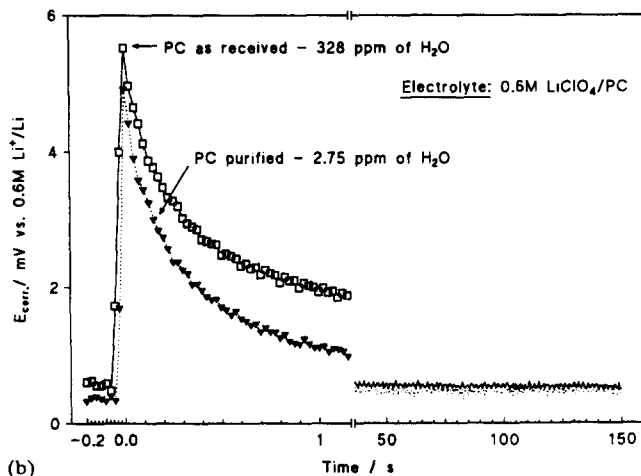


Fig. 2. Corrosion potential-time transients for lithium cutting in purified 0.6 M LiClO_4 /organic solvent electrolytes: (a) the first in situ cut; (b) the fourth in situ cut, and (c) the seventh in situ cut [12].



(a)



(b)

Fig. 3. The influence of water on the corrosion-time transients in (a) 0.6 M LiClO_4 /tetrahydrofuran and (b) propylene carbonate solvents.

that from the bromide ions on the surface. Concurrently, the signal from $(\text{CH}_3)_4\text{N}^+$ rose to a maximum at the pzc (Fig. 4). It appears that such bulky cations, with

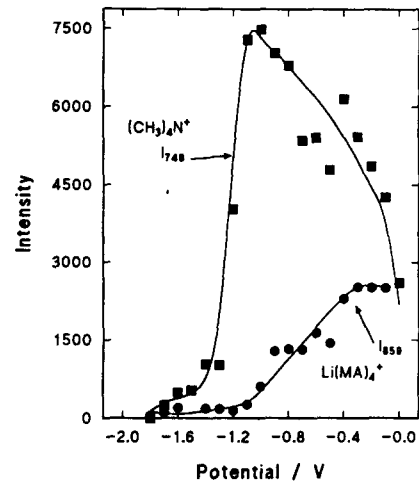


Fig. 4. Integrated intensities of the 859 cm^{-1} band of $\text{Li}(\text{MA})_4^+$ and the 748 cm^{-1} band of $(\text{CH}_3)_4\text{N}^+$ versus the applied electrode potential. The direction of potential change was from 0 to -2.0 V .

their charge virtually 'buried' inside the organic shell, behave as uncharged molecules. Possibly they cycle on and off the surface to level the effect of the lithium cycle.

The consequence of saturating the solution with CO_2 is illustrated in Fig. 5. At -0.4 V , a band at 1082 cm^{-1} is present after saturation with CO_2 ; it is absent when CO_2 is not introduced, although in one series of experiments it could be seen weakly at potentials more negative than -0.6 V . This band arises from the symmetric stretching mode of carbonate anion; it is the most intense band in the Raman spectrum of CO_3^{2-} , and is forbidden in the infrared spectrum; it is not to be confused with the $\nu_3(E')$ mode at about 1400 cm^{-1} , which is allowed and is intense in the infrared spectrum [22]. This band was observed at 1085 cm^{-1} from a silver electrode in PC/LiI [23]; its position is cation sensitive [24]. We can thus conclude that a carbonate species or film exists on the electrode surface and CO_2 facilitates its formation. As shown in Fig. 6, the CO_3^{2-}

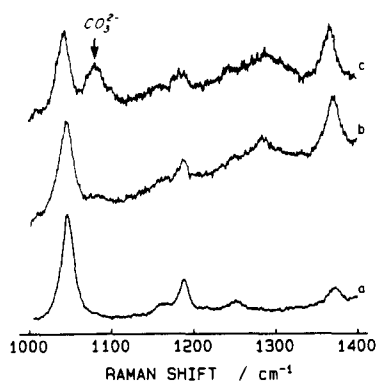


Fig. 5. Raman spectra in the 1000–1400 cm^{-1} region from a silver electrode surface in contact with 0.1 M LiAsF_6 , 0.005 M $(\text{CH}_3)_4\text{NBr}$, MA: (a) before the oxidation/reduction cycle; (b) -0.4 V with no addition of CO_2 , and (c) -0.4 V and saturation with CO_2 ; the signal at 1082 cm^{-1} from carbonate is marked.

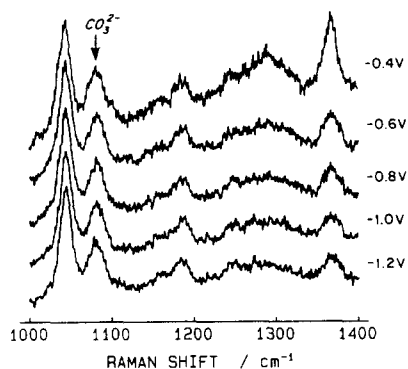


Fig. 6. Raman spectra as in Fig. 5(c) for the electrode at the designated voltages.

signal remains strong throughout the potential range from -0.4 to -1.2 V. For PC solvent systems, Fourier-transform infrared spectroscopy (FT-IR) has been used to confirm the presence of surface carbonate films such as ROCO_2Li [25,26]. Overtone and combination bands are less intense in Raman spectra, compared to infrared, and thus Raman spectra may be easier to interpret. In situ sample techniques are also easier to achieve using Pyrex glass windows and cells [4].

3.4. Intercalation of lithium into carbon-coke electrodes

Alternatives to metallic lithium are being sought to improve the cycleability of rechargeable lithium batteries based on organic electrolytes [27]. Carbon-based electrodes have received considerable attention and several recent reviews of the progress exist [28,29]. The Raman spectrum of highly ordered pyrolytic graphite (HOPG) contains a strong E_{2g} band at 1582 cm^{-1} , and other bands at 42 cm^{-1} (E_{2g}) and 2732 cm^{-1} [28,30]. The 1582 cm^{-1} band is the first-order scattering from the in-plane zone-centered E_{2g} mode, from materials with large intraplanar (L_a) and interplanar (L_c) microcrystallite dimensions [28,31,32]. It is shown by

Everall et al. [32] that laser-induced sample heating can significantly shift the E_{2g} vibrational mode of graphite to lower frequencies. It broadens and shifts to higher frequency with decreasing L_a and L_c [28]. When the intraplanar microcrystallite distance (L_a) decreases, as in glassy carbon, a new feature at 1360 cm^{-1} is observed. Its appearance has been linked to the breakage of symmetry occurring at the edges of graphite sheets. The more edges present, the more phonons that can result in Raman scattering [28]. Others have attributed this band to increased disorder in carbon [31,33]. Tuinstra and Koenig [34] reported that the ratio of the $1360/1580$ cm^{-1} integrated peak intensities is inversely proportional to the intraplanar microcrystallite distances L_a , determined crystallographically. Bowling et al. [35] have correlated this ratio for highly ordered pyrolytic graphite with electron transfer kinetics for the ferri-ferrocyanide redox system. Nikiel and Jagodzinski [36] have recently cast doubt on the generality of the correlation. Intercalation of guest species into a host structure of carbon strongly affects position, shape, and intensity of the E_{2g} band at 1582 cm^{-1} . The magnitudes of the changes in these parameters are strongly dependent upon the acceptor/donor properties of intercalant and the stage of the intercalation process [37].

Carbon-coke¹ electrodes sealed in polypropylene holders have been fabricated. (Teflon is unstable with respect to lithium and to dry non-aqueous solvents [38].) Raman spectra have been measured successfully of ethylene propylene diene monomer, EPDM binder, and the electrodes, ex situ and in situ in 1.2 M LiAsF_6/PC electrolyte, under potential and environmental control using the Raman microscope. The spectra are sensitive to sample preparation. We found that the band width (full width at half-maximum, FWHM) changes from 20 to 40 cm^{-1} on surface polishing; intraplanar microcrystallite sizes, L_a , decrease from 287 Å for untreated samples to about 30 Å for intensively polished electrodes. This latter value is in good agreement with earlier data of Nikiel and Jagodzinski [33]; they reported L_a equal to 35 Å for an oxidized nuclear grade carbon [33].

Raman spectra recorded before charging (B) and after the second charge (A) are illustrated in Fig. 7. The increase in intensity at 1353 cm^{-1} suggests a decrease in L_a from a very large value to about 108 Å. Raman lines of PC in the 1350 cm^{-1} region can interfere with these measurements; however, the intensity from these was not significant because it was possible to focus the laser on the surface through a bubble of evolved gas, thus reducing the intensity from the solvent. The PC bands at 1458 and 1486 cm^{-1} are

¹ This aspect of the work has been done in collaboration with J.J. Murray and R.S. McMillan of the Institute for Environmental Chemistry, National Research Council, Ottawa.

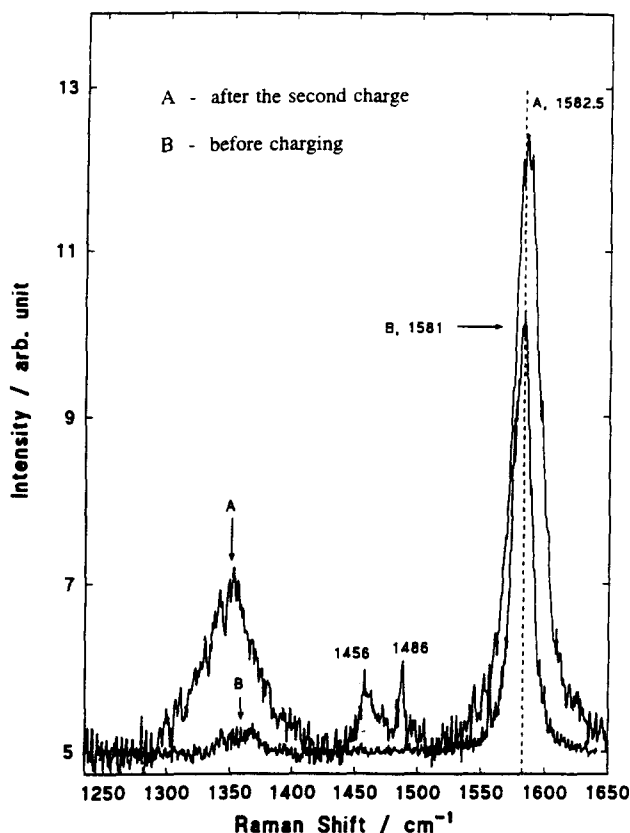


Fig. 7. Comparison of the Raman spectra of the carbon-coke electrode before and after charging, recorded in situ with the Raman microscope. (A) Electrode polished with 600 grit, and laser focussed through a gas phase, at the end of the second charge (after 93 h); laser power 7 mW. (B) Electrode polished with 600 grit, before charging; laser power 3 mW.

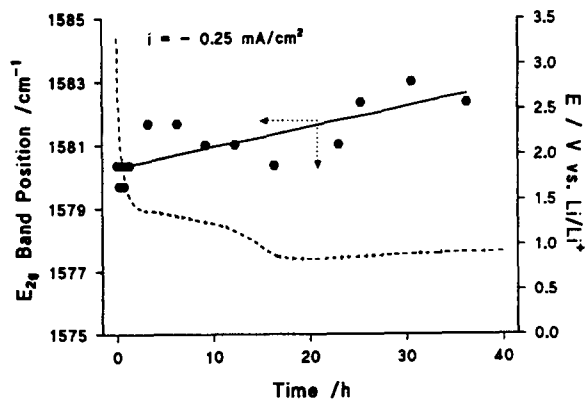


Fig. 8. Changes of the E_{2g} band position during the first charging process. The potential-time behaviour for a current of -0.25 mA cm^{-2} is shown by the dotted line.

much more intense than those in the 1350 cm^{-1} region; their weakness confirms the claim. The E_{2g} band shifts to higher frequencies during the charging process (Fig. 8) and the FWHM increases markedly at the beginning of charging and again at the point of potential arrest (Fig. 9). The frequency upshift is contrary to that observed when lithium (vapour) is introduced into the

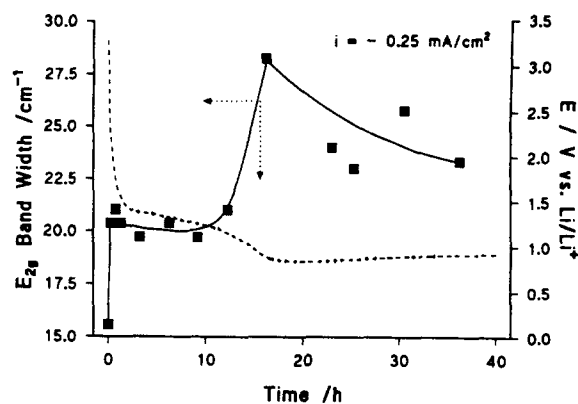


Fig. 9. Changes in the full width at half-maximum (FWHM) of the E_{2g} band during the first charging process.

highly ordered pyrolytic graphite; there, a mode softening was observed for increasing intercalate concentration [36,39,40]. This difference probably can be attributed to the co-intercalation of solvent, carried into the lattice by the lithium ions. It is like the upshift arising from acceptor compound intercalates [36,41]. Our work on this project is still at an early stage; however, the results suggest that electrochemical intercalation causes intraplanar rupturing, thus reducing the microcrystallite size and causing measurable disorder.

Acknowledgement

This work was supported by grants from the Natural Sciences and Engineering Research Council of Canada.

References

- [1] D.E. Irish and T. Ozeki, in J.G. Grasselli and B.J. Bulkin (eds.), *Analytical Raman Spectroscopy*, Wiley, New York, 1991, Ch. 4, p. 59.
- [2] M. Moskovits and D.P. DiLella, in R.K. Chang and T.E. Furtak (eds.), *Surface Enhanced Raman Scattering*, Plenum, New York, 1982, p. 243.
- [3] Z. Deng and D.E. Irish, *Can. J. Chem.*, **69** (1991) 1766.
- [4] Z. Deng and D.E. Irish, *Langmuir*, **10** (1994) 586.
- [5] Z. Deng and D.E. Irish, *J. Chem. Soc., Faraday Trans.*, **88** (1992) 2891.
- [6] P.V. Huong and J.P. Roche, in M. Grosmann, S.G. Elkomoss and J. Ringeissen (eds.), *Molecular Spectroscopy of Dense Phases*, Elsevier, Amsterdam, 1975, p. 613.
- [7] J. Barthel and R. Dresser, *J. Solution Chem.*, **23** (1994) 1133.
- [8] S. Hyodo and K. Okabayashi, *Electrochim. Acta*, **34** (1989) 1551, 1557.
- [9] R.L. Birke, T. Lu and J.R. Lombardi, in R. Vama and J.R. Selman (eds.), *Techniques for Characterization of Electrodes and Electrochemical Processes*, Wiley, New York, 1991, Ch. 5, p. 211.
- [10] B. Pettinger, in J. Lipkowski and P.N. Ross (eds.), *Adsorption of Molecules at Metal Electrodes*, VCH, New York, 1992, Ch. 6, p. 285.

- [11] M. Odziemkowski and D.E. Irish, *J. Electrochem. Soc.*, **139** (1992) 3063.
- [12] M. Odziemkowski and D.E. Irish, *J. Electrochem. Soc.*, **140** (1993) 1546.
- [13] S.A. Campbell, C. Bowes and R.S. McMillan, *J. Electroanal. Chem.*, **284** (1990) 195.
- [14] D. Aurbach, M. Daroux, P. Faguy and E.B. Yeager, *J. Electroanal. Chem.*, **297** (1991) 225.
- [15] D. Aurbach and A. Zaban, *J. Electrochem. Soc.*, **141** (1994) 1806.
- [16] E. Plichta, M. Salomon, S. Slane, M. Uchiyama, D. Chua, W.B. Ebner and H.W. Lin, *J. Power Sources*, **21** (1987) 25.
- [17] E. Plichta, M. Salomon, S. Slane and M. Uchiyama, *J. Solution Chem.*, **16** (1987) 225.
- [18] M. Salomon, S. Slane, E. Plichta and M. Uchiyama, *J. Solution Chem.*, **18** (1989) 977.
- [19] M. Salomon, M. Uchiyama, M. Xu and S. Petrucci, *J. Phys. Chem.*, **93** (1989) 4374.
- [20] M. Salomon, *J. Power Sources*, **26** (1989) 9.
- [21] N. Margalit and P.E. Krouse, *US Patent No. 4 160 070* (1979).
- [22] A.R. Davis and B.G. Oliver, *J. Solution Chem.*, **1** (1972) 329.
- [23] I.R. Hill, D.E. Irish and G.F. Atkinson, *Langmuir*, **2** (1986) 752.
- [24] M.H. Brooker and J.B. Bates, *J. Chem. Phys.*, **54** (1971) 4788.
- [25] D. Aurbach, Y. Gofer, M. Ben-Zion and P. Aped, *J. Electroanal. Chem.*, **339** (1992) 451, and refs. therein.
- [26] D. Aurbach, Y. Ein-Ely and A. Zaban, *J. Electrochem. Soc.*, **141** (1994) L1.
- [27] D. Fauteux and R. Koksang, *J. Appl. Electrochem.*, **23** (1993) 1.
- [28] R.L. McCreery, in A.J. Bard (ed.), *Electroanalytical Chemistry*, Vol. 17, Marcel Dekker, New York, 1991, p. 221.
- [29] J.R. Dahn, A.K. Sleigh, H. Shi, B.M. Way, W.J. Weydanz, J.N. Reimers, Q. Zhong and U. von Sacken, in G. Pistoia (ed.), *Lithium Batteries—New Materials, Developments, and Perspectives*, Elsevier, New York, 1994.
- [30] R.J. Nemanich, G. Lucovsky and S.A. Solin, *Solid State Commun.*, **23** (1977) 117.
- [31] R. Vidano and D.B. Fischbach, *J. Am. Ceram. Soc.*, **61** (1978) 13.
- [32] N.J. Everall, J. Lumsdon and D.J. Christopher, *Carbon*, **29** (1991) 133.
- [33] L. Nikiel and P.W. Jagodzinski, in W. Kiefer, M. Cardona, G. Schaack, F.W. Schneider and H.W. Schrötter (eds.), *Proc. 13th Int. Conf. on Raman Spectroscopy*, Wiley, New York, 1992, p. 782.
- [34] F. Tuinstra and J.L. Koenig, *J. Chem. Phys.*, **53** (1970) 1126.
- [35] R.J. Bowling, R.T. Packard and R.L. McCreery, *J. Am. Chem. Soc.*, **111** (1989) 1217.
- [36] L. Nikiel and P.W. Jagodzinski, *Carbon*, **31** (1993) 1313.
- [37] M.S. Dresselhaus and G. Dresselhaus, *Adv. Phys.*, **30** (1981) 139.
- [38] J. Barthel, M. Wühr, W. Sauerer and B. Hefer, *J. Electrochem. Soc.*, **140** (1993) 6.
- [39] P.C. Eklund, G. Dresselhaus, M.S. Dresselhaus and J.E. Fischer, *Phys. Rev. B*, **21** (1980) 4705.
- [40] M. Zanini, L.-Y. Ching and J.E. Fischer, *Phys. Rev. B*, **18** (1978) 2020.
- [41] C. Underhill, S.Y. Leung, G. Dresselhaus and M.S. Dresselhaus, *Solid State Commun.*, **29** (1979) 769.